

Supporting information

Superior Impact Toughness and Excellent Storage Modulus of Poly (lactic acid) Foams

Reinforced by Shish-Kebab Nanoporous Structure

Lihong Geng^{1,2,3}, Lengwan Li¹, Haoyang Mi², Binyi Chen², Priyanka Sharma³, Hongyang Ma³,

Benjamin S. Hsiao³, Xiangfang Peng^{1,2}, Tairong Kuang^{1,2*}*

¹National Engineer Research Center of Novel Equipment for Polymer Processing, The Key Laboratory of Polymer Processing Engineering of Ministry of Education, South China University of Technology, Guangzhou, 510640, PR China

²Department of Industrial Equipment and Control Engineering, School of Mechanical & Automotive Engineering, South China University of Technology, Guangzhou, 510640, PR China

³Department of Chemistry, Stony Brook University, Stony Brook, NY11794-3400, USA

*Corresponding Authors

Xiangfang Peng, Email: pmxfpeng@scut.edu.cn;

Tairong Kuang, Email: ktrmonarch0914@gmail.com

Supporting Information Table of Content

Figure S1. Schematic diagram of loop oscillating push-pull molding device.

Figure S2. Schematic diagram of Foaming Process.

Figure S3. Preparation process of samples for SEM observation.

Figure S4. 1D-SAXS curves of LOPPM-PLA in skin layer.

Figure S5. 2D-WAXD analysis of LOPPM-PLA foams

Figure S6. TGA thermogram curves

Figure S7. DSC thermograms for LOPPM and LOPPM-PLA foams.

Figure S8. Crystallinity of LOPPM-PLA and LOPPM-PLA foams.

Figure S9. DSC thermograms curves of LOPPM-PLA foam at different soaking temperature.

Experimental Section

PLA (4032D) with a molecular weight (Mw) of 207 kDa and a density of 1.24 g/cm³ was purchased from Nature Works (USA). The standard type I dumbbell PLA samples were first prepared using self-designed loop oscillating push-pull molding (LOPPM),¹ referred to as “LOPPM-PLA”, the schematic diagram and processing procedure is presented in Figure S1. Plungers 1 and 2 are connected using a rigid connecting rod to maintain the volume of the molding cavity constant. The push-pull cylinder drives Plungers 1 and 2 in a push-pull movement. The oscillating movement occurs when the oscillation unit works. In this study, both push-pull cylinder and the oscillating unit work. The intensive shear flow induces the formation of the shish-kebab during the processing of the PLA. The push-pull velocity V is 3.5 mm/s, oscillation amplitude A is 0.6 mm, and oscillation frequency f is 10 Hz.

For comparison, the regular PLA samples were also prepared using conventional injection molding (CIM), termed “CIM-PLA”.

Samples prepared by LOPPM were foamed in a homemade batch foaming device. Differing from conventional SC-CO₂ foaming processes, the LOPPM-PLA samples were soaked at a temperature far below melting temperature. The procedure of SC-CO₂LTFP was shown in Figure S2 and the sample was named “LOPPM-PLA foam”. Initially, LOPPM-PLA samples were put into a homemade batch foaming device. The vessel was heated to the desired temperature (T) ranging from 110 °C to 150 °C and pressurized to the supercritical carbon dioxide (SC-CO₂) of 20 MPa. The temperature and pressure were maintained for 2 h to allow SC-CO₂ to reach a saturation state. Subsequently, the vessel was cooled to foaming temperature (90 °C) and kept for 30 min with constant pressure of 20 MPa. Finally, the vessel was depressurized to ambient pressure in order to

induce pore nucleation and growth, followed by cooling to the room temperature through cycling water. For CFP, the soaking temperature was close to melting temperature, and hence crystal was melted and large pore size was obtained. For LTFP, the LOPPM-PLA samples were soaked at a temperature below melting temperature ranging from 110 °C to 150 °C. At this range, the crystal structure was maintained and the formed pores occupied amorphous regions.

Characterization

The LOPPM-PLA samples were freeze fractured along the flow direction, and the freeze fractured surfaces were etched with a water-methanol (1:2 v/v) mixture solution containing 0.025 mol/L NaOH for 12 h to remove amorphous regions. The LOPPM-PLA foams were freeze fractured directly in liquid nitrogen, as indicated in Figure S3. After coating the samples with a thin gold film, the different skin and core morphologies were observed with a field-emission Scanning Electron Microscope (SEM, Nano 430, FEI, USA).

2D-SAXS and WAXD patterns were obtained using the BL16B1 beamline at Shanghai Synchrotron Radiation Facility to examine crystal structures. 2D patterns were collected by an X-ray detector (Model Mar165, 2048 pixels × 2048 pixels of 80 μm × 80 μm). The distance between sample and detector was 1820 mm for SAXS and 136 mm for WAXD, respectively, and the wavelength was 0.124 nm. The orientation parameter of PLA molecules was characterized using Herman's orientation factor (f_H).²

$$f_H = \frac{3(\cos^2 \varphi)_{hkl} - 1}{2} \quad (1)$$

$$(\cos^2 \varphi)_{hkl} = \frac{\int_0^{\pi/2} I(\varphi) \cos^2 \varphi \sin \varphi d\varphi}{\int_0^{\pi/2} I(\varphi) \sin \varphi d\varphi} \quad (2)$$

Where $I(\varphi)$ is the scattering intensity along azimuthal angle φ . Azimuthal intensity distributions of the diffraction patterns were determined at $q = 10.67 \text{ nm}^{-1}$, corresponding to (200)/(110) planes. These were calculated at the azimuthal angle ranging from 0° to 180° .

The mechanical properties of the CIM-PLA, LOPPM-PLA and LOPPM-PLA foam samples were obtained using a pendulum impact testing machine (SANS ZBC1000) at room temperature according to ISO 180 standard. The dynamic mechanical properties were measured on a dynamic mechanical analyzer (DMA242C, NEZSCH) in a flexural mode with a frequency of 1 Hz over a temperature ranging from 30°C to 120°C at a heating rate of $3^\circ\text{C}/\text{min}$.

The melting behavior was analyzed using DSC (DSC204C, Netzsch Group, Bavaria, Germany) under nitrogen atmosphere. The endothermal curves of LOPPM-PLA and LOPPM-PLA foams prepared at different soaking temperature were recorded during heating from 25 to 190°C at a rate of $10^\circ\text{C}/\text{min}$.

Thermogravimetric analysis was performed on a TA SDT-Q600 (USA). PLA pellets, LOPPM-PLA and LOPPM-PLA foam were heated from room temperature to 500°C . The residual weight was recorded as a function of temperature. Weight loss starting temperature (T_{onset}), maximum-speed weight loss temperature (T_{max}) and weight loss ending temperature (T_{offset}) were analyzed.

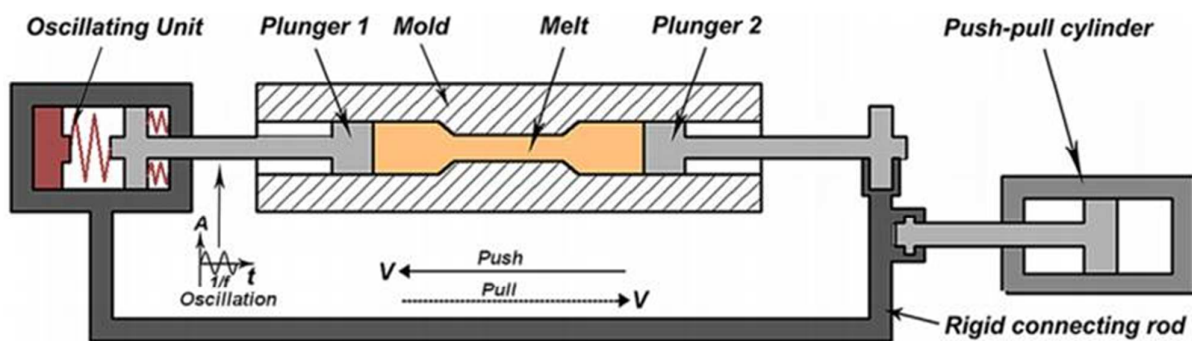


Figure S1. Schematic diagram of loop oscillating push-pull molding device.

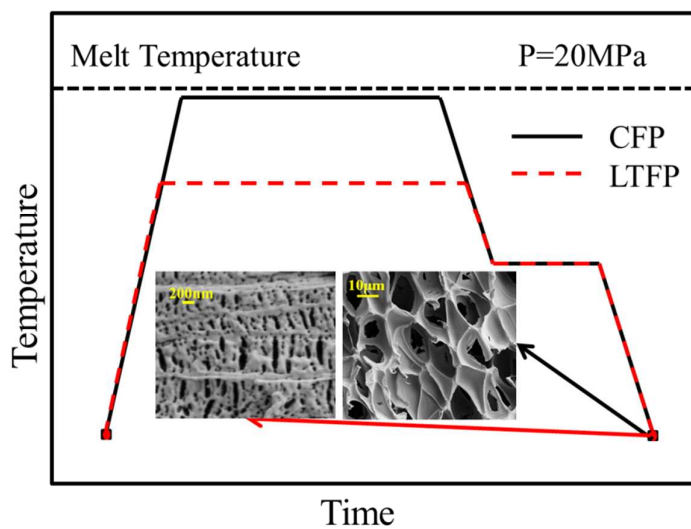
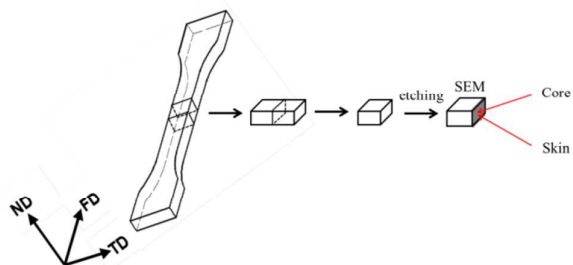


Figure S2. Schematic diagram of Low Temperature Foaming Process (LTFP) and Conventional Foaming Process (CFP).

LOPPM-PLA



LOPPM-PLA foam

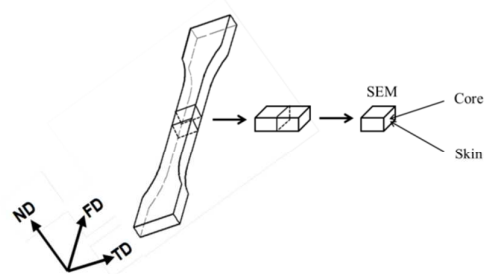


Figure S3. Preparation process of LOPPM-PLA and LOPPM-PLA foam samples for SEM observation.

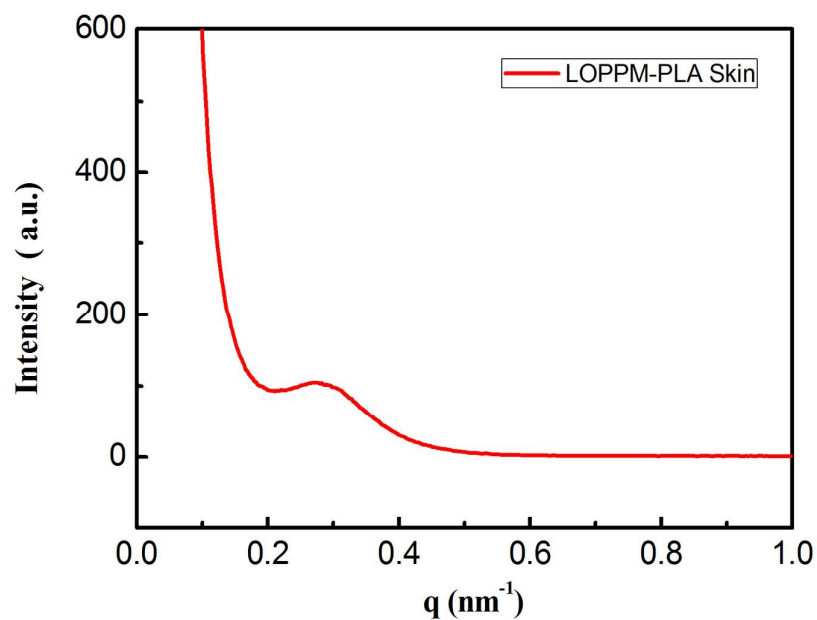


Figure S4. 1D-SAXS curves showing the corresponding intensity profile of the scattering pattern of LOPPM-PLA in skin layer.

The integrated intensity $I(q)$ ($q = 4\pi\sin\theta/\lambda$) was calculated by integrating in the angular range over the whole kebab pattern, where 2θ represents the scattering angle and λ represents the wavelength of the X-ray.

The long period was calculated according to Bragg's equation $L = 2\pi/q^*$, where L represents the long period and q^* represents the peak position in 1D- $I(q)$ scattering curve. In this study, q^* of LOPPM-PLA skin was 0.2691 nm^{-1} corresponding to the long period L of 23.35 nm.

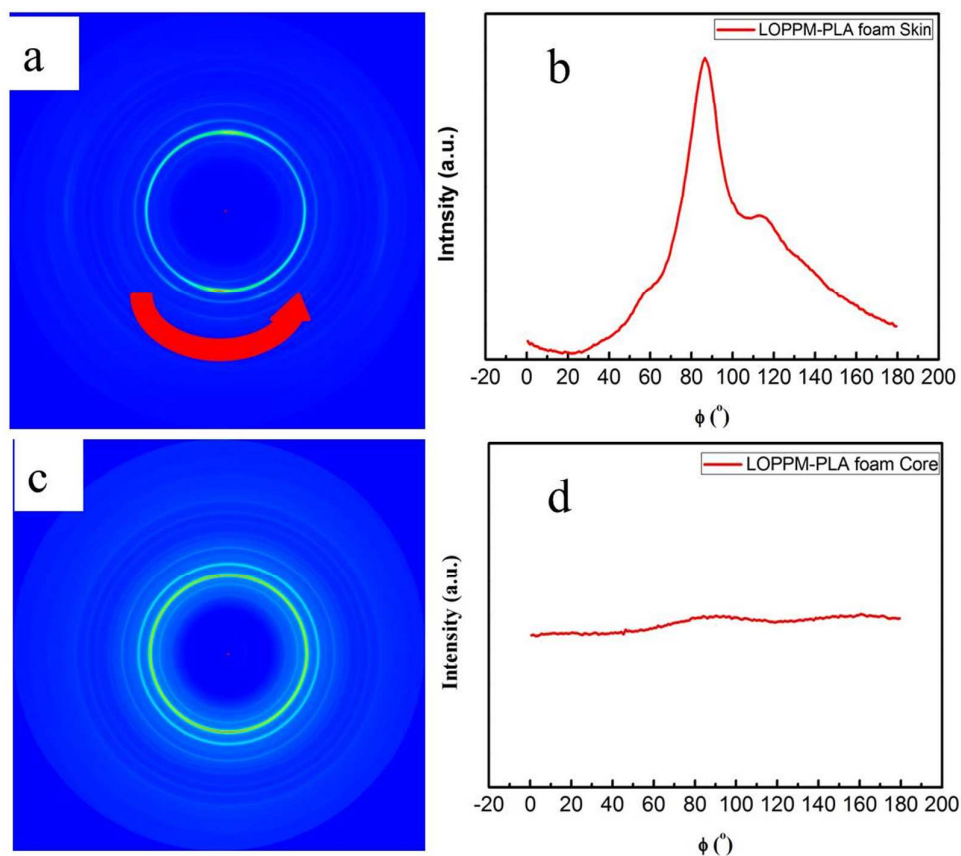


Figure S5. 2D-WAXD pattern (a) and azimuthal intensity distribution(b) of LOPPM-PLA foams in skin layer; 2D-WAXD pattern (c) and azimuthal intensity distribution(d) of LOPPM-PLA foams in core layer.

The azimuthal integration pictures indicate that the shish-kebab structure in the skin layer is oriented along the flow direction because of intensive shear force (Herman's orientation factor is 0.36), while the crystal structure is random in the core layer without intensive shear force (Herman's orientation

factor is 0). Compared to the azimuthal intensity distributions of LOPPM-PLA in the skin layer (Figure 1b and 1c, Herman's orientation factor is 0.31), the degree of orientation of LOPPM-PLA foams increased because more amorphous PLA chains recrystallized along the existing oriented shish-kebabs.

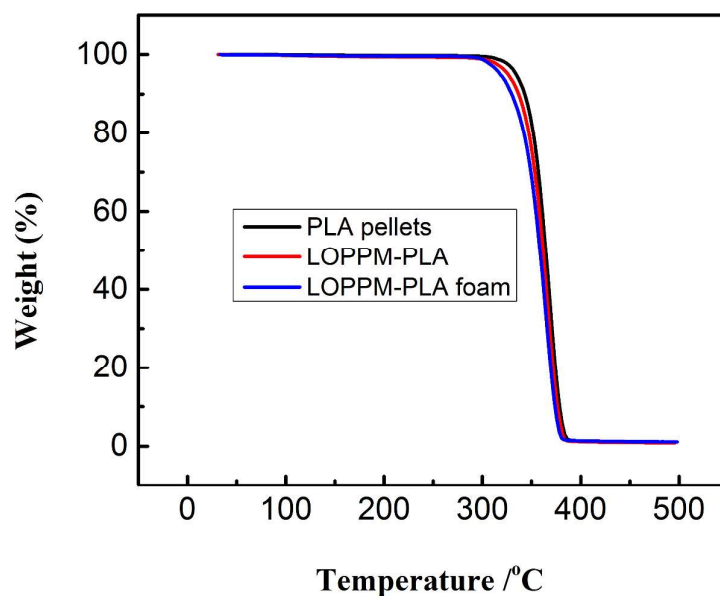


Figure S6. TGA thermogram curves of PLA pellets, LOPPM-PLA and LOPPM-PLA foam.

Table S1. TGA characteristics of PLA pellets, LOPPM-PLA and LOPPM-PLA foam

Samples	T_{onset} (°C)	T_{max} (°C)	T_{offset} (°C)
PLA pellets	346.3	344.0	341.0
LOPPM-PLA	372.7	369.2	362.7
LOPPM-PLA foam	380.6	378.5	376.0

T_{onset} : weight loss starting temperature, T_{max} : maximum-speed weight loss temperature, T_{offset} : weight loss ending temperature

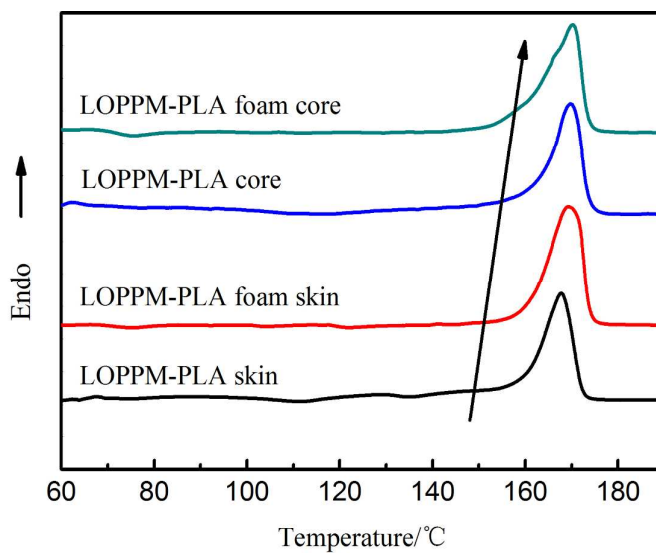


Figure S7. DSC thermograms for LOPPM and LOPPM-PLA foam samples.

The melting temperature of LOPPM-PLA was determined by DSC measurement. In order to maintain the crystal structure during foaming, the soaking temperature should be below the melting temperature ranging from 110 °C to 150 °C.

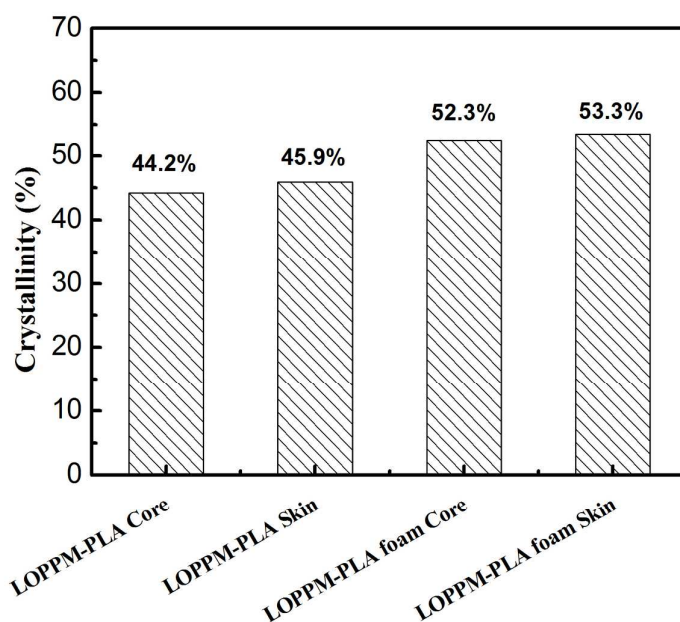


Figure S8. Compared crystallinity of LOPPM-PLA and LOPPM-PLA foams.

Crystallinity (X_c) of non-foamed and foamed samples was calculated according to DSC thermograms. Crystallinity is equal to the ratio of measured melting enthalpies and the melting enthalpy of 100% crystalline PLA (taken as 93.6 J/g).³

For LOPPM-PLA sample, the crystallinity in the skin layer was larger than that in the core layer because of applied intensive shear force, which induced crystallization. After foaming, the crystallinity of LOPPM-PLA foams was larger compared to LOPPM-PLA due to the recrystallization during soaking.

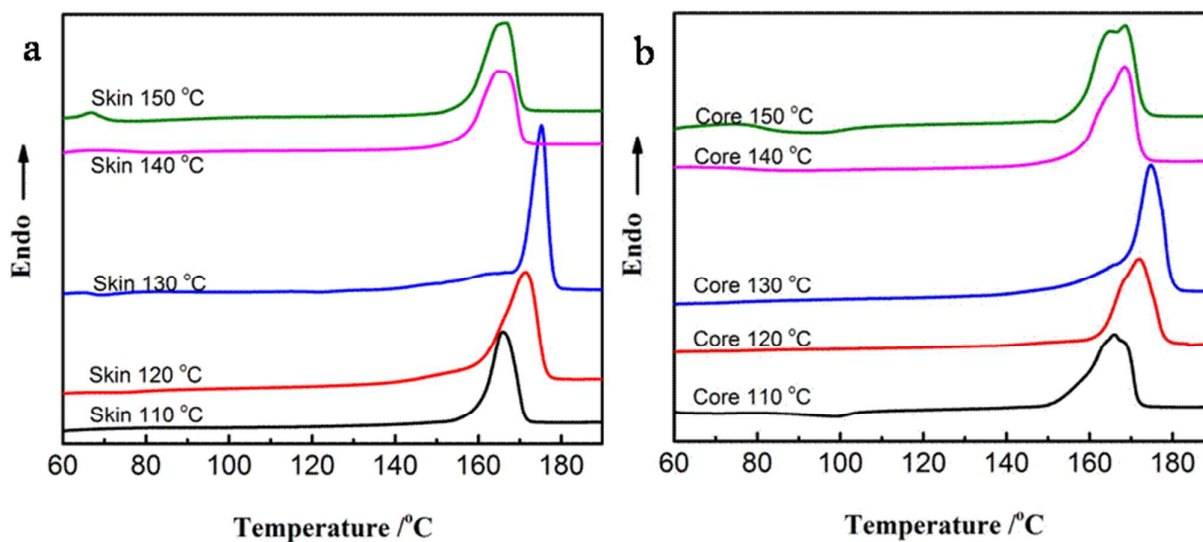


Figure S9. DSC thermograms curves of skin (a) and core (b) layer for LOPPM-PLA foam samples at different soaking temperature.

Table S2. DSC characteristics of for LOPPM-PLA foam samples at different soaking temperature.

Soaking	Skin		Core	
Temperature (°C)	T_m (°C)	X_c (%)	T_m (°C)	X_c (%)
110	165.4	45.2	166.3	44.0
120	171.4	53.3	172.1	52.3
130	175.2	54.1	174.7	52.4
140	166.2	49.1	168.7	48.5
150	166.8	42.7	168.5	44.4

T_m : melting temperature, X_c : crystallinity

References

- (1) Peng, X.; Chen, J.; Kuang, T.; Yu, P.; Huang, J., Simultaneous Reinforcing and Toughening of High Impact Polystyrene with a Novel Processing Method of Loop Oscillating Push–Pull Molding. *Mater. Lett.* **2014**, *123*, 55-58.
- (2) Zhou, S. Y.; Huang, H. D.; Ji, X.; Yan, D. X.; Zhong, G. J.; Hsiao, B. S.; Li, Z. M., Super-Robust Polylactide Barrier Films by Building Densely Oriented Lamellae Incorporated with Ductile in Situ Nanofibrils of Poly(Butylene Adipate-Co-Terephthalate). *ACS Appl. Mater. Interfaces* **2016**, *8*, 8096-8109.
- (3) Wu, D.; Cheng, Y.; Feng, S.; Yao, Z.; Zhang, M., Crystallization Behavior of Polylactide/Graphene Composites. *Ind. Eng. Chem. Res.* **2013**, *52*, 6731-6739.